The Journal of Experimental Biology 205, 1531–1545 (2002)
Printed in Great Britain © The Company of Biologists Limited 2002
JEB3775

The locust tegula: kinematic parameters and activity pattern during the wing stroke

Hanno Fischer[1,*], Harald Wolf[2] and Ansgar Büschges[3]

[1]*School of Biology, Bute Medical Buildings, University of St Andrews, St Andrews, Fife KY16 9TS, Scotland,* [2]*Neurobiologie, Universität Ulm, D-89069 Ulm, Germany* and [3]*Zoologisches Institut, Universität Köln, Weyertal 119, D-50923 Köln, Germany*

*e-mail: hf4@st-andrews.ac.uk

Accepted 15 March 2002

Summary

The tegula is a complex, knob-shaped sense organ associated with the base of the locust wing. Despite a detailed knowledge of its role in flight motor control, little is known about the relationship between the stroke parameters of the wing, movement of the tegula organ and the pattern of tegula activity. In this study, therefore, the kinematic parameters of the fore- and hindwings were investigated with respect to the tegula activity pattern during tethered flight. The following results were obtained. (i) The tegula moves through a complex three-dimensional trajectory during the wing stroke, involving inclination and rotation about its longitudinal axis. (ii) The kinematic parameters of tegula movement are phase-locked to the wing stroke and vary in conjunction with wing stroke parameters such as amplitude and cycle period. (iii) In accordance with these phase-locked kinematics, both the onset of tegula activity with respect to the downstroke (latency) and the discharge of the organ (burst duration and amplitude) vary in conjunction with downstroke movement and cycle period, resulting in an (almost) constant phase of tegula activation during the stroke cycle. (iv) The pattern of tegula activity during flight is largely independent of stroke amplitude. (v) The latency, burst duration and amplitude of tegula activity are strongly related to the angular velocity of the wing during the downstroke, with latency reaching a steady minimum value at higher angular velocities. The data suggest that the tegula encodes the timing and velocity of the downstroke and that it may be involved in the control of the stroke's angular velocity.

Key words: locust, sensorimotor system, tegula, insect, flight, wing stroke parameter, wing hinge element, *Locusta migratoria*.

Introduction

In most animals, the generation of functional motor patterns for the repetitive movement of the body, limbs or wings during locomotion relies both on pattern generators in the central nervous system and on peripheral sensors, which provide feedback to the locomotor control circuitry (for a review, see Büschges and El Manira, 1998). In locust flight, for example, the proprioceptive sense organs associated with the wings, such as stretch receptors, campaniform sensilla and tegulae, have been shown to contribute to the generation and modulation of the flight motor command (Gettrup, 1966; Wendler, 1974; Möhl, 1985; Wolf and Pearson, 1987b, 1988; Reye and Pearson, 1988). The locust tegulae, knob-shaped sense organs at the anterior base of the wings (Kniazeva, 1970), have been investigated in particular detail, mostly with regard to the sensorimotor pathways involved in flight pattern generation. During flight, tegula input contributes mainly to the timing of wing elevation (Wolf and Pearson, 1988; Pearson and Wolf, 1989; Wolf, 1993), while nerve recordings indicate that the tegula organs are excited during the (preceding) downstroke of the wing (Neumann, 1985; Wolf and Pearson, 1988; Fischer and Ebert, 1999).

Contrasting with the rather detailed information available about tegula sensorimotor pathways, little is known about the functional morphology of the tegula organs or their mode of activation. The tegula is composed of two types of mechanosensor, an external hair plate located on the cupola, which contains approximately 40 sensory hairs, and a chordotonal organ inside the cupola, which consists of approximately 30 scolopidial sensilla (Kutsch et al., 1980). While single (filiform) hairs are typical exteroreceptors responsive to the degree and direction of hair bending (for reviews, see Thurm, 1982, 1984), hair plates (e.g. Kent and Griffin, 1990; Mücke, 1991; Newland et al., 1995) or hair rows often subserve a proprioceptive function, for example in monitoring joint position and movement (e.g. Wong and Pearson, 1976; Pflüger et al., 1981; Dean and Wendler, 1983; Bässler, 1983). This is achieved through the successive deflection of adjacent hairs by skeletal elements such as neighbouring limb segments. Chordotonal organs (for a review, see Matheson, 1990) are typical proprioceptors responsive to the (relative) position and movement of skeletal

elements, including acceleration and vibration (e.g. Zill, 1985; Hofmann and Koch, 1985; Kittmann and Schmitz, 1992; also in tympanal organs, Yack and Fullard, 1993). In addition, chordotonal organs are employed to monitor the position and movement of an appendage in the context of motor control (e.g. Burns, 1974; Field and Pflüger, 1989; Matheson and Field, 1995; Büschges, 1994).

The tegula would be equipped to encode almost every parameter of the locust wing stroke important for aerodynamic force production, flight control and steering (amplitude and angular velocity of the wing stroke, e.g. Lehmann and Dickinson, 1998; timing of the stroke reversals, e.g. Dickinson et al., 1999). The tegula is also involved in phase-tuning muscle activity during the wingbeat cycle, particularly regarding the wing elevators (Wolf and Pearson, 1988; Pearson and Wolf, 1989; Wolf, 1993, Fischer and Ebert, 1999). Since the activation phase is one of the key features controlling the mechanical output of synchronous oscillatory insect muscles (e.g. Josephson, 1985; Stevenson and Josephson, 1990), this would provide a direct functional context for wingbeat-synchronous mechanosensory pathways, such as that of the tegula, in flight pattern generation.

In the present study, we examined the functional morphology of the tegula organs, their timing and activity pattern during the wing stroke and possible stroke parameters encoded by the tegula. In a videographic analysis, the relationship between wing movement and tegula kinematics (including the kinematics of selected wing hinge elements) was examined, and electrophysiological and wing movement recordings were combined to analyse the relationship between tegula discharge and wing stroke parameters. The data suggest that the tegula does not just signal the downstroke movement, but rather monitors details of stroke timing and the angular velocity of the wing.

Materials and methods

Animals and preparations

Adult female locusts (*Locusta migratoria* L.) were used for all experiments 6–12 days after the imaginal moult. Experiments were performed at 25–30 °C. The animals were attached to a holder by the ventral meso- and metathoracic sterna using beeswax resin. The tarsi of all legs were removed to avoid termination of flight episodes by tarsal contact. Flight was induced by short wind puffs onto the frons or cerci.

For high-speed video analysis, the tegula organs (encircled in Fig. 1A,B, which shows electron microscographs of the location of the tegula organs, the main structural components of the wing base and the pterothorax) were marked with circular dots of black ink (Texpen, USA, marked with open arrows in Fig. 1D) under a dissection microscope as a reference point for the examination of kinematic parameters. Ink dots were placed centrally on the organs, without covering the posterior hair fields of the tegulae or touching other structures of the wing base. To allow video recording of the forewing tegula, the posterior edge of the pronotum had to be clipped without damaging the ligament between the pro- and mesothorax.

For electrophysiological experiments, a flight preparation was used (Wolf and Pearson, 1987a) in which the animal was glued to the holder in an inverted position. A flap of the ventral cuticle was removed to provide access to either the mesothoracic or the metathoracic ganglion and to the proximal segments of nerve 1 (N1; nomenclature after Campbell, 1961).

Aspects of functional morphology were studied either in freshly killed animals or in isolated pterothoraces, macerated in concentrated KOH, to investigate cuticular anatomy (see Pfau and Koch, 1994). Anatomical descriptions are based on Albrecht (1953).

Data acquisition

A commercially available digital high-speed video system (HSVS; hardware: Weinberger Systems, Switzerland; software; Speedcam, Fraunhofer Institute, Erlangen, Germany) was used which allows synchronous recording by two separate cameras (frame frequency adjustable between 1 and 1000 frames s^{-1}). Tegula movement was recorded from the dorsal side with one camera (Sigma macrophoto lens, f=90 mm, Fig. 1D); the other camera was equipped with a zoom telephoto lens (Cosimar, f=1.4–50 mm) and recorded the stroke movements of the fore- and hindwings from a lateral view (not shown). The frames of both cameras were system-internally synchronised during recording. Between the two cameras, frames corresponding in time were identifiable by the displayed frame numbers. Recordings were stored on-line on computer disc. For analysis, the digitally recorded episodes of both cameras were transferred onto VHS videotape. In each individual, the lengths of the fore- and the hindwings (base to tip) were measured, and the dimensions of wing hinge components and tegula organs were determined with an ocular micrometer after the experiments.

Flight motor activity was monitored by bipolar electromyographic (EMG) electrodes (30 μm stainless-steel pins) from the first basalar depressor (forewing, M97; hindwing, M127) and a tergosternal elevator (M83/84 and M113, respectively; nomenclature according to Snodgrass, 1929) (Fig. 2Ai,Bi). To record tegula activity, bipolar hook electrodes were placed either on nerve N1 or on nerve branch N1C (nomenclature after Campbell, 1961), which contains the afferent axons from the wing base. The recording site was isolated with silicone grease. In this experimental arrangement, wing position during flight was recorded by an optical position detector (von Helversen and Elsner, 1977) (Fig. 2Ai,Bi) in parallel with the extracellular nerve recordings. For each animal, the detector was calibrated by positioning the wing passively at given stroke angles after the experiment. In addition, after the completion of electrophysiological recordings, the recorded tegula organ was severed as a control (Fig. 2Aii,Bii). The data were stored on compact disc (CD recorder, Pioneer PDR 04) and transferred onto a computer hard disc using an analog/digital converter (Biologic DRA-800).

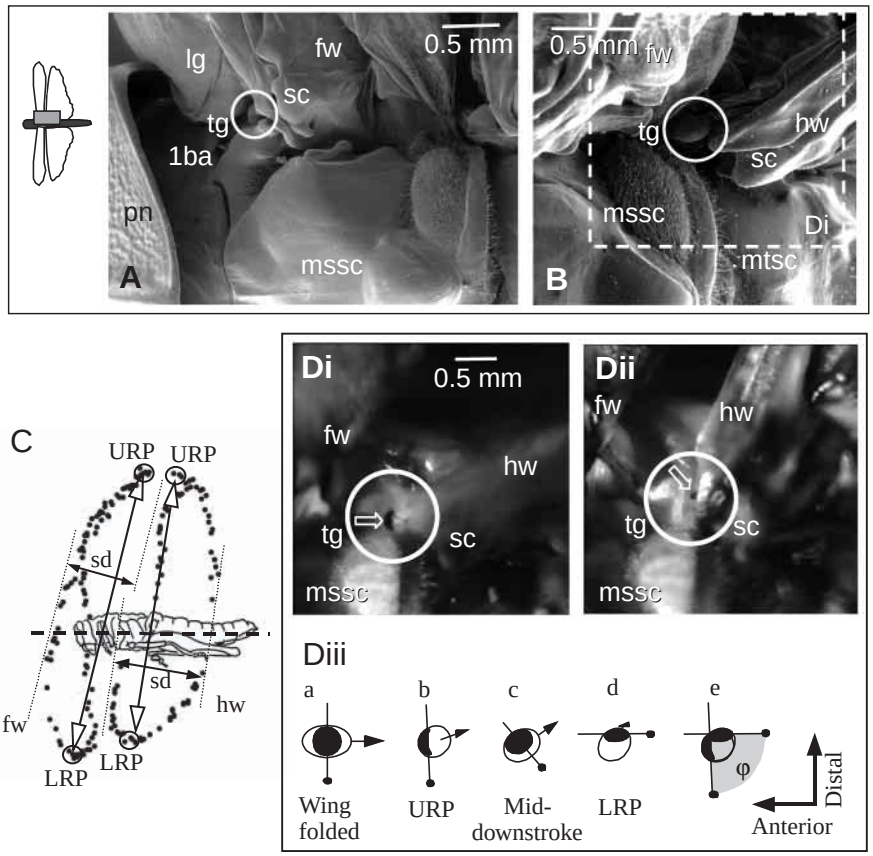

Fig. 1. Location of the tegula. Electron microscographs showing dorsal views of the mesothoracic (A) and metathoracic (B) wing hinge of an adult female *Locusta migratoria*. The locations of the tegula organs are circled; orientation and wing hinge area are indicated by the locust outline (left; lower image margin, body midline). (A) The location of the forewing tegula (tg) in the downstroke position, with the organ located in a fold of the subcostal (sc) membrane; (B) the hindwing organ in the upstroke position. fw, forewing; hw, hindwing; lg, ligament; 1ba, anterior process of the first basalar sclerite; mssc, mesothoracic scutum (anterior border); mtsc, metathoracic scutum; pn, pronotum. (C) Schematic drawing of the wing tip (black dots) trajectories, reconstructed from the superimposed video frames recorded during three wingbeat cycles by the lateral camera. The upper (URP) and lower (LRP) reversal points of the forewing (fw) and the hindwing (hw) are indicated by open circles. sd, stroke deviation with respect to the stroke plane (indicated by the line connecting the URP and LRP). (D) Dorsal view of the metathoracic wing hinge; pictures are single frames from a high-speed video recording (500 frames s^{-1}). The tegula organ (circled) is shown in the upstroke (Di) and downstroke (Dii) position (approximate area shown in Di is indicated by the dashed frame in B). The tegulae were marked with black ink dots (open arrows). (Diii) Schematic drawing of the tegula in dorsal view, with the ink dot indicated in black, (a) when the wing was folded in the resting position, (b) at the upper reversal point (URP) of the wing, (c) in the horizontal wing position (mid-downstroke) and (d) at the lower reversal point (LRP) of the wing. The arrow indicates the longitudinal axis of the organ, pointing towards the wing tip. The instantaneous angle of tegula rotation was measured as the orientation of the small bisector (line marked by a dot) of the ink dot ellipsoid in the plane of view, with the orientation of the ellipsoid at the upper reversal point of the wing used as a reference. (e) Superposition of b and d showing the total angle of rotation during a wingbeat cycle (φ).

Data evaluation

The VHS recordings were monitored on a 27 inch Sony Trinitron colour video monitor. To measure wing stroke parameters, recordings by the lateral camera were screened frame by frame, and the instantaneous stroke position and stroke deviation (see Fig. 1C for explanation) were transferred to overhead transparencies for further analysis (see also Baker and Cooter, 1979). The distance between the upper and lower reversal points of the wing was measured, and the total (peak-to-peak) stroke amplitude (Φ, see also Sane and Dickinson, 2001) was calculated from these data as a cosine function of wing length (base to tip; see Fischer and Kutsch, 1999).

The pterothorax (i.e. the fused meso- and metathorax with fused sterna and pleura, which is further stabilised by several sternal and pleural apostemata; e.g. Albrecht, 1953) was studied after maceration by applying mechanical stress, which revealed rigidity along the longitudinal axis. Experiments in which the thorax was filmed during flight showed that, by using a ventral attachment of the locust by both meso- and metathoracic sterna (e.g. Zarnack and Wortmann, 1989), flight activity did not result in any longitudinal (i.e. foreward and backward) movements or lateral displacements of the pterothorax relative to the tether. The tether or the margin of the video frames was therefore used as a reference for measuring movements of the tegula and other skeletal elements of the wing hinge. In contrast, suspension of the animals by the pronotum (e.g. Dugard, 1967; Baker, 1979) resulted in strong oscillatory displacement of the body relative to the tether during flight and, thus, prevented accurate focusing on the tegulae and other wing structures.

The degree of tegula rotation in the wingbeat cycle was estimated from the transparencies, according to Fig. 1Diii, with the orientation of the ink dot at the upper reversal point of the wing serving as a reference. Initially, this procedure was tested using a Styrofoam sphere marked with a circular ink dot and rotated through known angles while being filmed from the same view as the tegula during experiments. The degree of tegula inclination (i.e. the inclination of its longitudinal axis) was estimated by measuring the relative changes in the visible area of the ink dot using the area of the dot at the upper reversal point of the wing as a reference. For individual calibration, the wing was positioned at given angles in quiescent locusts before flight experiments.

The evaluated parameters of wing stroke and tegula activity

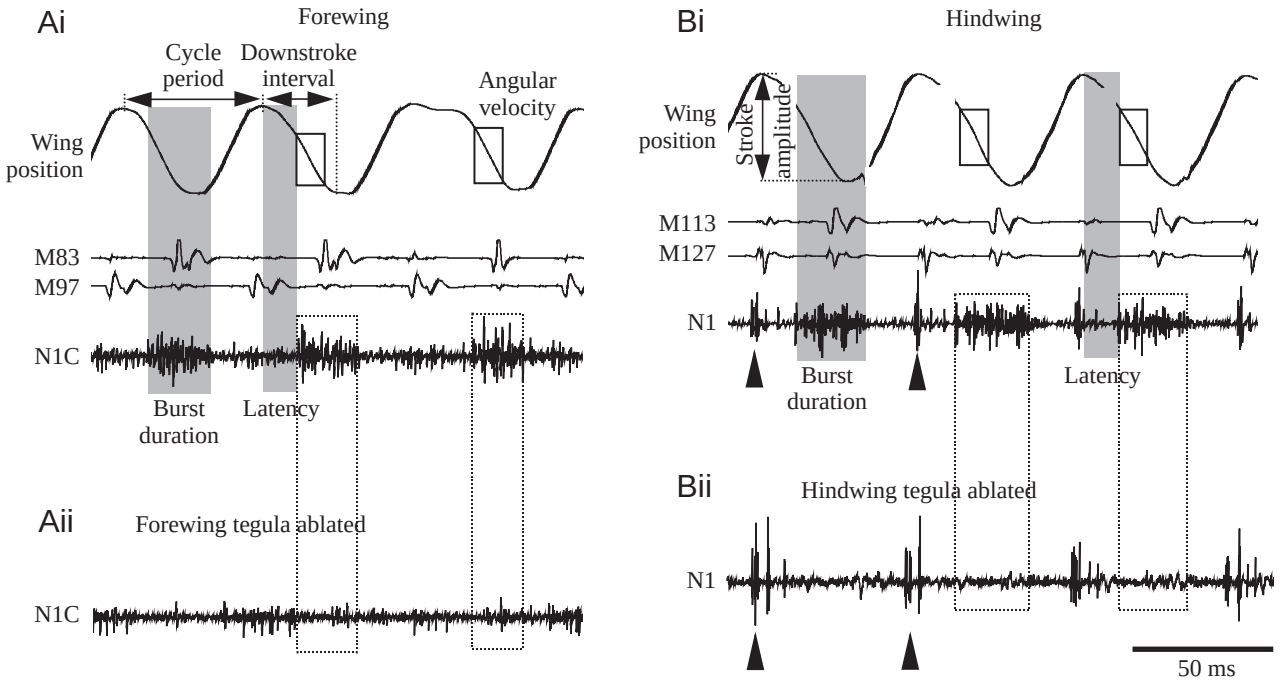

Fig. 2. Discharge pattern of the forewing (A) and hindwing (B) tegula in relation to wing position during tethered flight. Wing position (top traces in i) was monitored by an optical position detector. Tegula activity (bottom traces) was recorded extracellularly from nerve branches N1 (B) or N1C (A) (details in Pearson and Wolf, 1988), which supply the tegula organs. Black arrowheads indicate cross-talk between motoneurons innervating the dorsal longitudinal depressor muscles. Electromyographic (EMG) recordings were made from wing depressor (M97, M127) and elevator (M83, M113) muscles. Shaded areas indicate tegula burst duration and latency (time between onset of wing downstroke and start of tegula discharge). Cycle period was determined as the time between consecutive downstroke movements. The downstroke interval was measured between the beginning and end of the downstroke movement. Stroke amplitude was determined from the distance between the upper and lower reversal points of the wing. The angular velocity of the wing (ω, rad s^{-1}) was calculated from the change in wing position during the 10 ms period following tegula activation (indicated by the open boxes in Ai and Bi). The phase of onset of tegula activity within a cycle was calculated as latency divided by cycle period. (Aii,Bii). Nerve recordings after ablation of the tegula organs recorded in Ai and Bi (traces selected and aligned according to EMG activity, which is not shown).

are explained in the legend to Fig. 2. The mean amplitude of the tegula discharge was calculated as the integral of the rectified tegula burst divided by burst duration (e.g. Chau et al., 1998). The data were analysed using the Spike 2 data software package (Cambridge Electronics, UK) and the DataView signal-analysis program (W. J. Heitler, University of St Andrews, UK).

Statistical analyses

Statistical analyses were computer-aided (KaleidaGraph, MS Excel, StatView) and followed the criteria described by Sachs (1978). Correlation and linear regression analyses were tested for significance levels of $P<0.05$, with r indicating the linear correlation coefficient. Partial correlation coefficients (r^*) were determined according to Sachs (1978). The statistical significance of non-linear regressions of data is given by the coefficient of determination, r^2. Mean phase values are given as $\phi \pm$ mean angular deviation, with **r** describing the mean vector. Circular two-sample comparison was performed using the Watson–Williams test (Batschelet, 1981). Unless stated otherwise, data are given as mean ± S.D.

Results

The results described in the following two sections were obtained by high-speed video recordings (500 frames s^{-1}) from 10 different animals, five investigating the forewing and five the hindwing structures. Three to five flight episodes were evaluated per animal.

Kinematic parameters of thoracic structures and wing hinge sclerites surrounding the tegula

The cupola of the tegula organ is integrated into a common ligament attached to the scutum, basalar sclerite, pleura and leading edge of the wing. This is illustrated for the forewing in Fig. 3A. The schematic forewing diagram in Fig. 3B shows that, during the downstroke, the scuta of the wing segments moved dorsally but were also displaced posteriorly along the body axis. During this posteriorly directed movement of the scutum, the wing was promoted, i.e. shifted in the anterior direction (anterior stroke deviation, see Fig. 1C). The changes in stroke position and stroke deviation of the wing were strictly phase-coupled during the wingbeat cycle (Fig. 3C; at the upper reversal point, the wing tip has reached its posterior extreme position; the anterior extreme position is reached when the

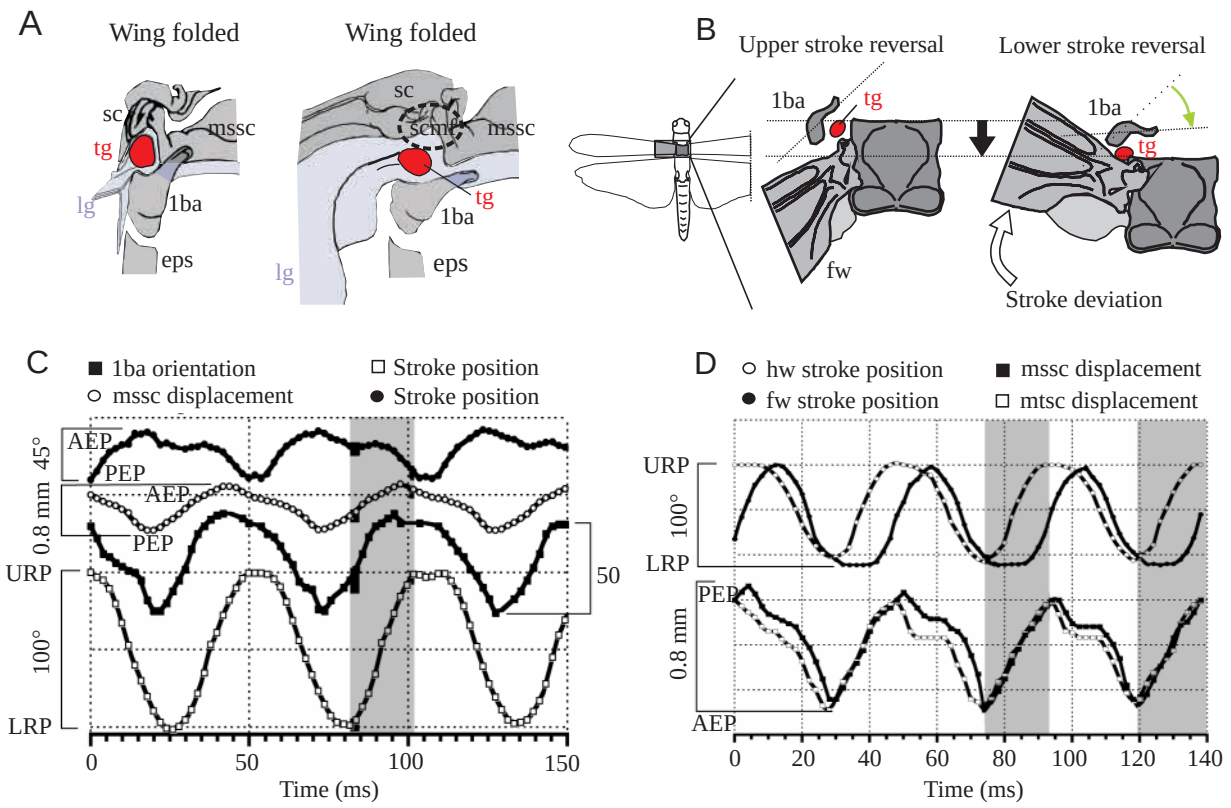

Fig. 3. Morphology and movement of the wing hinge area. (A) Tegula position in the folded (left) and unfolded (right) forewing, frontal view. mssc, mesothoracic scutum; mtsc, metathoracic scutum; tg, tegula; lg, ligament; 1ba, first basalar sclerite; eps, episternum; sc, subcosta; scmf, subcostal membrane fold (also for B–D). The tegula is integrated into a common ligament (lg, blue shading) attached to the basalar sclerite, scutum, subcosta and leading edge of the wing. During the downstroke, the organ slides into a subcostal membrane fold, indicated by a dashed circle (see Fig. 1Diii). (B) Schematic drawing of the forewing hinge in dorsal view (the diagram on the left indicates the area shown). The posterior displacement of the scutum (black arrow) and synchronous rostral stroke deviation (white arrow) of the wing near the lower stroke reversal are indicated by reference lines; the change in the orientation of the first basalar sclerite is indicated by a green arrow. See text for details. fw, forewing. (C) Displacement of mesothoracic wing hinge components during the wingbeat cycle; three consecutive cycles are shown. The upstroke phase of the forewing is indicated by the shaded area. AEP, anterior extreme position of movement; PEP, posterior extreme position of movement; URP, upper reversal point; LRP, lower reversal point of the wing (see also Fig. 1C). (D) Displacements of the meso- and metathoracic scuta in relation to fore- (fw) and hindwing (hw) movements; three consecutive wingbeat cycles are shown. The upstroke of the hindwing is indicated by the shaded areas.

wing passes through the lower reversal point). This appears to be due to the tight mechanical coupling between most elements of the wing hinge (Pfau, 1982). The pterothoracic scuta are connected by an elastic ligament. Thus, during the downstroke, the two scuta moved posteriorly at slightly different times; during the upstroke, their anterior-directed movements were almost synchronous (and in phase with the hindwing upstroke, shaded area in Fig. 3D). Furthermore, both scuta also underwent a vertical displacement during the wingbeat cycle, roughly in anti-phase to the wing movement, because of their location on the inner side of the wing hinge. The scuta were displaced dorsally during the downstroke and returned ventrally during the upstroke. We were, however, unable to quantify this vertical movement because both scuta showed considerable dorso-ventral deformation superimposed on their vertical movements, which appeared to be caused mainly by the contraction of the dorsal longitudinal muscles.

In the video recordings taken from the dorsal side, the mesothoracic first basalar sclerite performed rotational, rather than horizontal, movements during the wingbeat cycle (determined *via* its horn-shaped anterior process, 1ba in Fig. 1; shown schematically in Fig. 3B using the orientation of the process at the upper reversal point of the wing as a reference). This is probably (i) because the first basalar depressor muscle attaches to the posterior part of the sclerite (Albrecht, 1953) and (ii) because the sclerite itself is attached to the scutum by the medial and anterior edges of the common ligament. The posteriorly and upward-directed components of the scutum movement, together with the contraction of the first basalar muscle during the downstroke, are thus transformed into an ‘inward rotation’ of the first basalar sclerite. This change in orientation was slightly phase-shifted with respect to the stroke position of the forewing [Fig. 3C, advanced by a mean phase (ϕ) of 0.18±0.03, **r**=0.967, *N*=45, data pooled from five animals] but occurred almost in synchrony with the horizontal movement component of the scutum (ϕ=0.02±0.02, **r**=0.945,

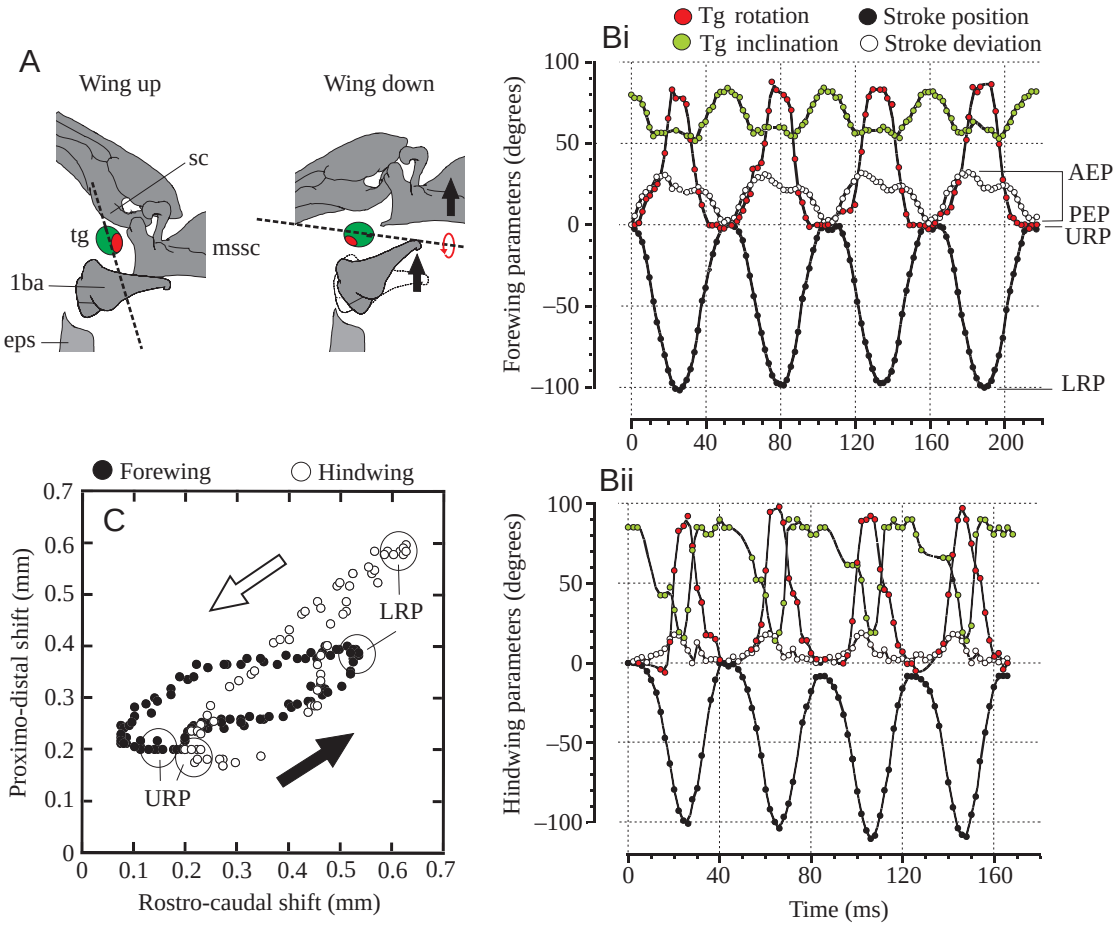

Fig. 4. Movements of the tegula during the wingbeat cycle. (A) The forewing hinge in frontal view; schematic drawings of upper (left) and lower (right) stroke reversals. Abbreviations as in Fig. 3. The dashed line marks the longitudinal axis of the tegula organ; rotational movement around this axis is indicated by an elliptical red arrow. Black arrows indicate displacement of the scutum and the change in orientation of the basalar sclerite. (B) For four wingbeat cycles of the forewing (Bi) and the hindwing (Bii), the time courses of tegula rotation and inclination are shown in relation to stroke position and stroke deviation of the wing. (C) Displacement of the tegula organ in the horizontal plane during the wing stroke (data from four consecutive wingbeat cycles superimposed). The black arrow marks the direction of movement during the downstroke; the white arrow indicates upstroke. URP, upper reversal point; LRP, lower reversal point of the particular wing; AEP, anterior extreme position of movement; PEP, posterior extreme position of movement.

N=45). The first basalar sclerite of the hindwing could not be investigated because it is located below the plane of the hindwing and was not visible in the video recordings.

Kinematic parameters of the tegula organ in the wingbeat cycle

The tegula organ followed a complex three-dimensional trajectory during the wingbeat cycle in both the fore- and hindwings. During the downstroke, the longitudinal axis of the oval-shaped tegula was inclined horizontally. This is illustrated schematically for the forewing in Fig. 4A (the longitudinal axis of the organ is indicated by a dashed line). At the same time, the organ was rotated around its longitudinal axis (anti-clockwise on the animal's right-hand side, i.e. anterior margin upwards; indicated by the elliptical red arrow in Fig. 4A). During the upstroke, this movement was reversed; the longitudinal axis of the organ moved vertically, with a synchronous downward rotation of the anterior tegula margin.

The temporal pattern of tegula inclination and rotation, with respect to stroke position and deviation movements, is shown for four consecutive wingbeat cycles in Fig. 4B (forewing parameters in Fig. 4Bi and hindwing parameters in Fig. 4Bii; both panels represent typical experimental animals, data confirmed in all animals studied). Movements of the wing and tegula organ exhibited a stable phase relationship, with the tegula reaching maximum rotation (and minimum inclination) near the lower reversal point of the wing beat (right in Fig. 4A) and *vice versa* near the upper reversal point (left in Fig. 4A).

The mean values of inclination and rotation were lower in the forewing than in the hindwing organs ($P<0.05$, data not shown). For both tegulae, total inclination and rotation movements during a wingbeat cycle (determined as peak-to-peak values, Fig. 4B) were significantly correlated with wing

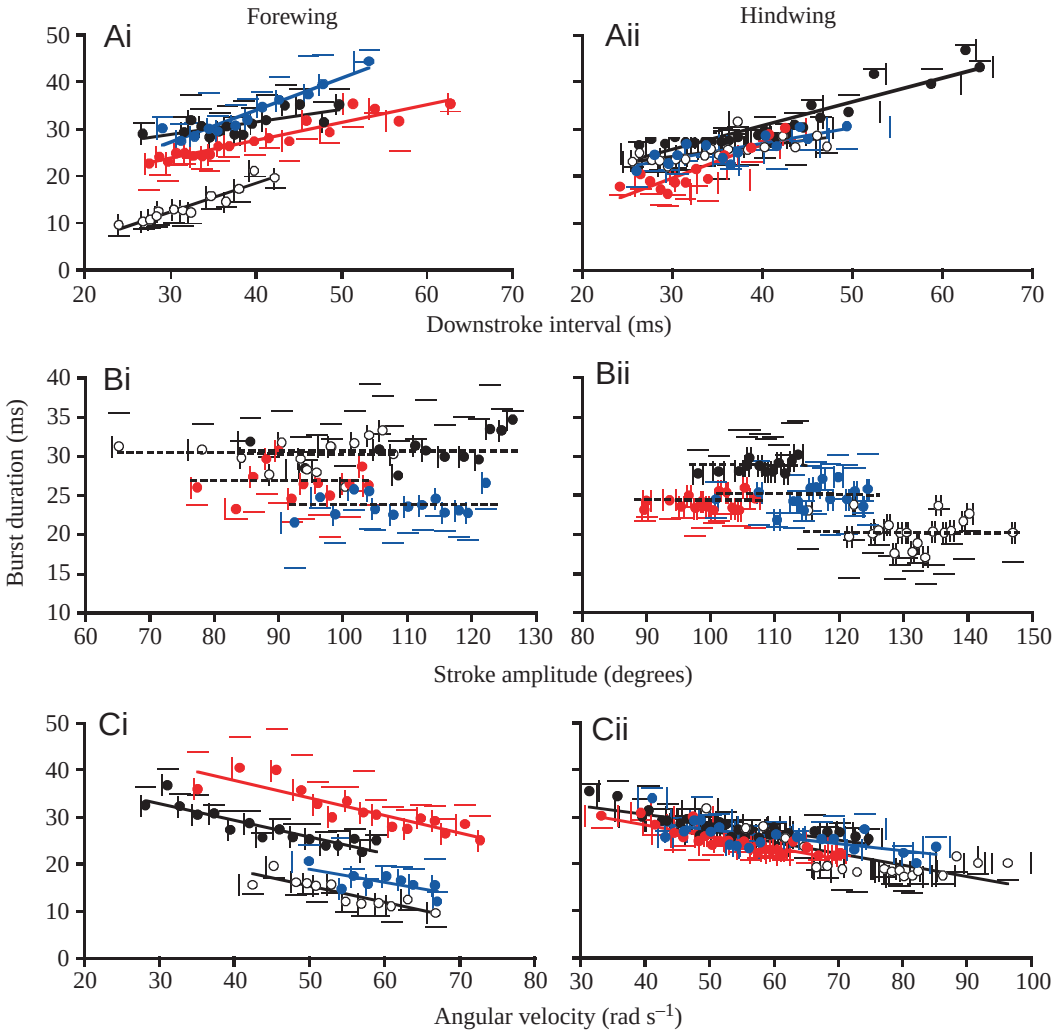

Fig. 5. Relationships between tegula burst duration and wing stroke parameters (see Fig. 2) for the fore- (i) and hindwing (ii) tegulae (data from four individuals shown, each given in a different colour). In both pairs of tegula organs, the burst duration depends on the duration of the downstroke interval (A) (P<0.05, regressions indicated by solid lines); however, burst duration is not significantly related to stroke amplitude (B) (P>0.05, regressions indicated by dashed lines). (C) Tegula burst duration is significantly related to the angular velocity during the downstroke (P<0.05). For each individual, data points represent means ± S.D. (indicated as caps of error bars only) calculated from 5–21 observations during 3–5 flight episodes. Relationships for all animals investigated are given in Table 1.

stroke amplitude in all animals investigated (0.66<r<0.73, P<0.05, N=10, data not shown). Furthermore, the angular velocity of tegula inclination and tegula rotation during a wingbeat cycle was significantly correlated with cycle period (0.68<r<0.83, P<0.05, N=10, not shown) and with the angular velocity of the wing itself (0.71<r<0.89, P<0.05, N=10, data not shown). These findings indicate that tegula movement reliably reflects wing movement, albeit slightly differently in the fore- and hindwings.

In addition to the rotational movements described above, the tegula organs of both pairs of wings shifted in the horizontal plane during the wingbeat cycle (Fig. 4C). During the downstroke, the tegulae were displaced posteriorly in synchrony with the posteriorly directed movement of the adjacent segmental scutum (Fig. 3) and the anterior stroke deviation. During the upstroke, these movements were reversed. The tegulae also showed a proximo-distal component of movement during the wingbeat cycle since the distance between the right and left thoracic pleurae decreased during the downstroke and increased during the upstroke (ordinate in Fig. 4C), this effect being more pronounced in the metathorax (open circles in Fig. 4C).

Pattern of tegula activity with respect to wing stroke parameters: burst duration

The pattern of tegula activity was investigated with respect to specific wing stroke parameters in 20 animals (10 for the forewing organs, 10 for the hindwing organs). For both pairs of wings, the relationships between stroke parameters and tegula burst duration are given in Fig. 5.

In the hindwing, mean tegula burst duration was 27.1±3.2 ms (N=10), which was slightly, although

Table 1. *Relationships between wing stroke parameters and tegula activity pattern during flight in* Locusta migratoria

Number	*N*	*la*(*di*)	*la*(Φ)	*la*(ω)	ϕ(*cp*)	ϕ(Φ)	ϕ(ω)	*bd*(*di*)	*bd*(Φ)	*bd*(ω)	*di*(*cp*)	ω(*cp*)	Φ(*cp*)
Forewing tegula													
1	67	r=0.64	r=0.62	r^2=0.35	NS	r=0.52	NS	NS	NS	r=–0.34	r=0.57	r=–0.34	r=0.39
2	85	r=0.85	NS	r^2=0.52	NS	NS	r^2=0.48	r=0.31	NS	NS	r=0.64	r=–0.44	r=0.37
3	145	r=0.92	NS	r^2=0.62	r=0.60	NS	r^2=0.49	r=0.71	NS	r=–0.68	r=0.91	r=–0.87	NS
4	80	r=0.76	r=0.49	r^2=0.59	r=0.45	r=0.48	r^2=0.48	r=0.61	r=0.34	r=–0.61	r=0.79	r=–0.65	NS
5	136	r=0.72	NS	r^2=0.48	NS	NS	NS	r=0.36	NS	r=–0.51	r=0.56	r=–0.49	NS
6	92	r=0.84	NS	r^2=0.46	r=–0.47	NS	r^2=0.49	NS	NS	r=–0.49	NS	NS	NS
7	49	r=0.72	NS	r^2=0.42	NS	NS	NS	r=0.36	r=0.41	NS	r=0.36	r=–0.55	NS
8	133	r=0.87	r=–0.30	r^2=0.75	NS	NS	r^2=0.36	NS	NS	r=–0.42	r=0.73	r=–0.81	r=–0.51
9	134	r=0.36	NS	r^2=0.42	r=0.40	r=0.42	r^2=0.38	r=0.26	NS	NS	NS	r=–0.28	NS
10	141	r=0.86	NS	r^2=0.62	NS	NS	NS	r=0.38	r=0.31	NS	r=0.36	r=–0.42	r=–0.33
Hindwing tegula													
1	129	r=0.61	NS	r^2=0.34	NS	NS	NS	r=0.41	r=–0.39	r=–0.44	r=0.51	r=–0.62	r=–0.57
2	90	r=0.78	NS	r^2=0.59	NS	NS	NS	NS	NS	NS	NS	NS	r=–0.36
3	142	r=0.65	r=–0.57	r^2=0.38	r=–0.29	r=0.30	NS	NS	NS	NS	NS	NS	r=–0.58
4	171	r=0.92	NS	r^2=0.84	r=0.34	r=–0.40	r^2=0.76	r=0.41	NS	r=–0.39	r=0.56	r=–0.65	r=–0.55
5	55	r=0.91	NS	r^2=0.84	NS	NS	r^2=0.62	r=0.45	NS	r=–0.37	r=0.81	r=–0.73	NS
6	95	r=0.86	NS	r^2=0.46	r=–0.38	NS	r^2=0.52	r=0.72	NS	r=–0.66	r=0.57	r=–0.63	NS
7	120	r=0.87	NS	r^2=0.78	r=0.42	NS	r^2=0.44	r=0.54	NS	r=–0.52	r=0.75	r=–0.74	NS
8	122	r=0.82	NS	r^2=0.69	NS	NS	NS	r=0.67	NS	r=–0.52	r=0.67	r=–0.57	NS
9	76	r=0.64	r=–0.61	r^2=0.60	NS	NS	NS	r=0.60	NS	r=–0.54	r=0.49	r=–0.49	NS
10	101	r=0.62	NS	r^2=0.52	NS	NS	NS	r=0.54	r=0.47	r=–0.47	r=0.61	r=–0.55	r=0.45

In the fore- and hind-wings, the relationships between tegula burst duration (*bd*), latency (*la*), phase of activity onset during the wingbeat cycle (ϕ), wing downstroke interval (*di*), wing stroke amplitude (Φ), angular velocity of the wing during the downstroke (ω) and cycle period (*cp*) were investigated in 10 animals (numbered 1–10).

N, number of observations; *r*, linear coefficient of correlation (P<0.05); r^2, coefficient of determination, given for non–linear relationships (P<0.01); r>0 indicates a positive and r<0 a negative correlation between the variables tested. NS, no significant relationship between the variables tested (P>0.05).

significantly, higher than the mean burst duration observed in the forewing organs (24.6±3.7 ms, P<0.05, N=10). In the majority of animals, and for both pairs of wings, the duration of tegula discharge was significantly related to the duration of the wing downstroke (P<0.05, forewing, 7/10 animals; hindwing, 8/10 animals; shown for four individuals in Fig. 5Ai,ii). A summary of the individual data is provided in Table 1. In the hindwing, burst duration increased, on average, by 0.36±0.18 ms per millisecond of increase in the downstroke interval (N=8), while in the forewing, the increase was 0.37±0.18 ms per millisecond (N=7). These values were not significantly different from one another (P>0.05). For the majority of these animals, the downstroke interval was correlated with cycle period (P<0.05, see Table 1). Thus, the duration of the tegula burst was also correlated with cycle period (P<0.05, data not shown). In the remaining (two and three, respectively) animals, burst duration was not significantly related to the downstroke interval (P>0.05).

In contrast, in the majority of animals, tegula burst properties were not correlated with stroke amplitude in either pair of wings (P>0.05; results shown for four individuals in Fig. 5Bi,ii). In the remaining animals, burst duration was either slightly negatively (one hindwing) or slightly positively (three forewings, one hindwing) correlated with stroke amplitude (see Table 1).

The duration of tegula bursts was significantly related to the angular velocity during the downstroke (ω, rad s^{-1}) in the majority of individuals (P<0.05; hindwing: 8/10 animals; forewing: 6/10 animals; data from four individuals each are shown in Fig. 5Ci,ii). Tegula burst duration decreased by 0.28±0.13 ms rad^{-1} s^{-1} (N=6), on average, in the forewing, and by 0.22±0.11 ms rad^{-1} s^{-1} (N=8) in the hindwing organ. The remaining (two and four, respectively) locusts exhibited no significant relationship between burst duration and angular velocity (P>0.05, Table 1).

Pattern of tegula activity: latency and phase of discharge onset

The tegula organs are activated with some delay after the beginning of the downstroke movement. In the hindwing, this latency was, on average, 15.5±2.6 ms (N=10); it was 11.6±4.1 ms (N=10) in the forewing. These two values are significantly different (P<0.05, N=10). In both sets of wings, the latency between the start of the downstroke and the onset of tegula activity was related to the stroke parameters examined above. The results are shown in Fig. 6. Latency was related to downstroke interval in all 20 animals examined

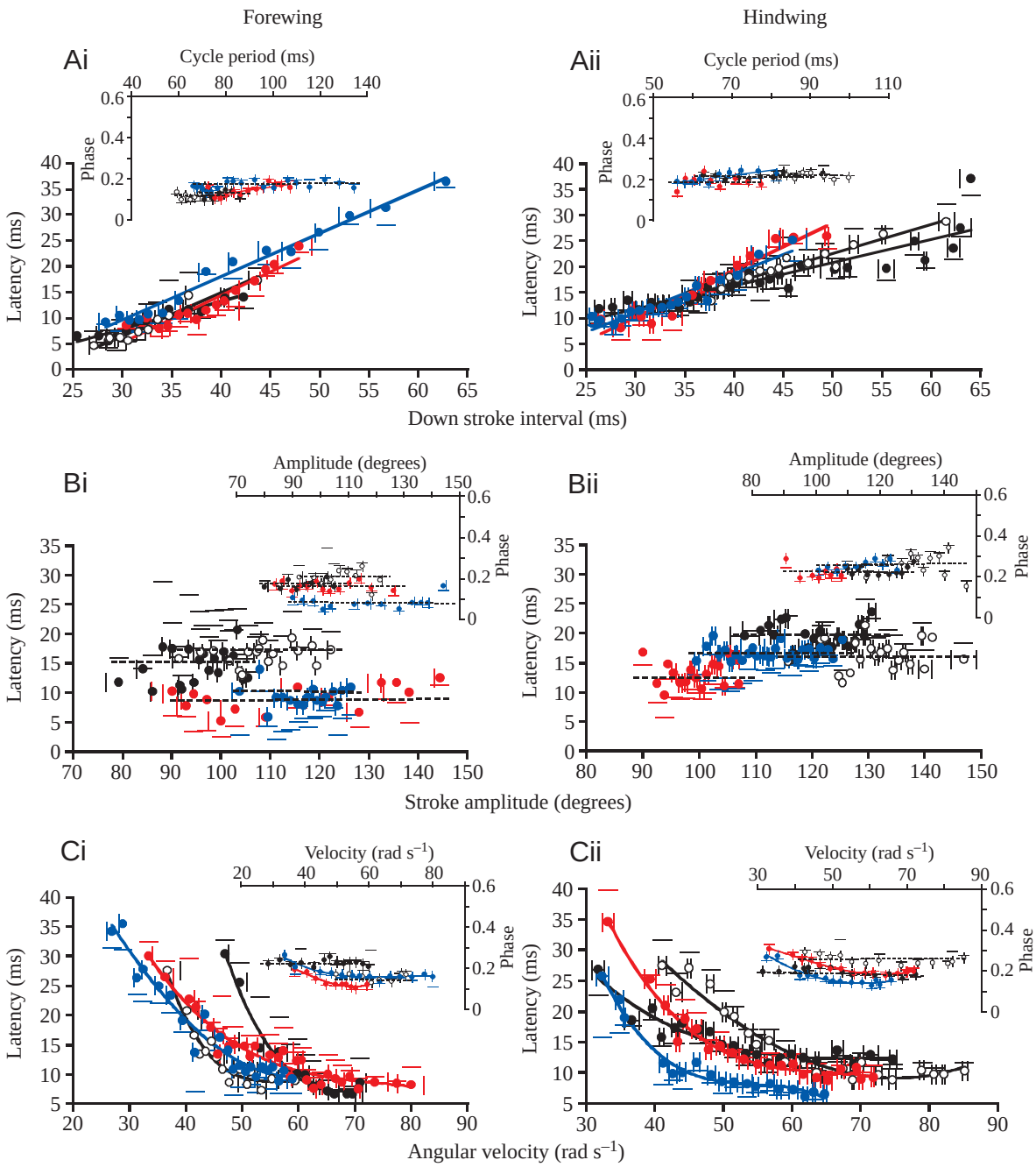

Fig. 6. Latency (main panels A–C) and phase (insets in A–C) of the onset of tegula activity in the wingbeat cycle and their relationship to wing stroke parameters (see Fig. 2) in the fore- (i) and hindwing (ii) (data from four individuals shown, each in a different colour). (A) In both pairs of sense organs, latency depends on the downstroke interval (P<0.05; solid regression lines). However, the phase of tegula activation was not related to cycle period (P<0.05; broken regression lines). (B) Neither the latency nor the phase of the tegula discharge depends on stroke amplitude (P>0.05). (C) The relationship between the latency of tegula activity and wing angular velocity is non-linear (r^2 significantly different from zero, P<0.01). Within the range of angular velocities observed, latency approaches or reaches a minimum value at higher angular velocities. In contrast, the phase of tegula discharge is almost independent of angular velocity. For details, see text. Relationships for all animals investigated are given in Table 1.

(P<0.05; Fig. 6A,Aii shows data from four individuals; see Table 1). In the hindwing, the latency increased by an average of 0.67±1.5 ms per millisecond increase in downstroke interval (N=10). Comparable values were observed in the forewing organ (0.72±1.9 ms ms^{-1}, mean values not significantly different, P>0.05, N=10). In contrast, latency was not significantly related to stroke amplitude for the forewing in seven out of 10 individuals and in the hindwing in eight out of 10 individuals (P>0.05; Fig. 6Bi,Bii illustrates data from four individuals; see Table 1). In the remaining animals, the

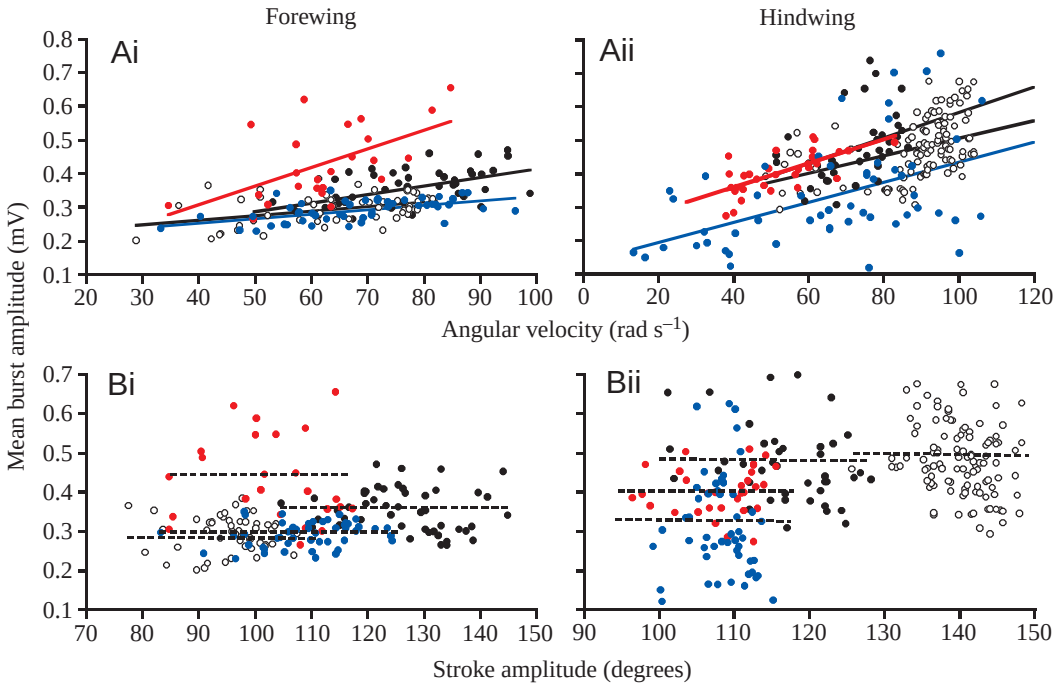

Fig. 7. Relationships between the mean amplitude of the tegula burst (calculated from rectified and integrated recordings) and the angular velocity (A) and stroke amplitude (B) of the fore- (i) and hindwings (ii) (data from four individuals shown, each in a different colour). In both pairs of sense organs, mean burst amplitude depends on the instantaneous angular velocity of the wing (A; solid regression lines), whereas burst amplitude is not significantly related to instantaneous stroke amplitude (B; broken regression lines). Data points represent samples pooled from 2–4 flight episodes. Data shown in A and B are from the same animals. For details, see text.

relationship between latency and stroke amplitude was not consistent: two locusts showed a positive relationship, the remaining three a negative relationship (P<0.05).

In all 20 animals investigated, the latency of tegula discharge was dependent on the angular velocity of the wing during the downstroke in a non-linear manner. For both the fore- and hindwing organs, the typical characteristics of latency, as dependent on angular velocity, are shown in Fig. 6Ci,ii (data from four animals; r^2 significantly different from zero in all animals investigated, P<0.01, Table 1). In seven of the 10 animals, the latency of hindwing tegula activation reached a minimum at approximately 66.5±9.2 rad s^{-1} (N=7). The corresponding minimum value was 60.7±5.9 rad s^{-1} (N=6) in the forewing organ, with six of the 10 animals reaching such a minimum (minimum values were calculated from the equations used to fit the data points). In the remaining seven animals, the graph did not reach a consistent minimum value within the angular velocities recorded.

In 12 of the 20 animals, the phase of the onset of tegula activity in the wingbeat cycle (insets Fig. 6) was not significantly correlated with the cycle period (P>0.05). The results were inconsistent among the remaining animals (positively correlated in five and negatively correlated in three individuals, see Table 1). Similarly, there was no clear relationship between the phase of tegula discharge and stroke amplitude in the majority of animals (15/20, Table 1; P>0.05, insets Fig. 6B). The findings that latency was inversely related to angular velocity and that this relationship, shown in Fig. 6C, was hyperbolic, suggest that the tegula is activated at a nearly constant phase irrespective of the wing's angular velocity. Indeed, in 10 of 20 animals, phase was not significantly correlated with angular velocity (P>0.05, Table 1). In the majority of the remaining animals, the phase of tegula activation varied little over a wide range of angular velocities (insets in Fig. 6C). Consistent with these observations, the mean coefficient of determination r^2 between phase and angular velocity (r^2_ϕ=0.29±0.06, N=20) was much lower than that between latency and angular velocity (r^2_{lat}=0.56±0.03, N=20, Table 1).

Pattern of tegula activity: mean burst amplitude

In 12 animals (six forewings, six hindwings), the 'mean amplitude' of the rectified and integrated tegula burst was calculated and related to instantaneous wing stroke parameters. In all 12 animals investigated, mean burst amplitude was correlated with the angular velocity of the wing (P<0.05, r ranging from 0.41 to 0.77 in the forewings and from 0.40 to 0.68 in the hindwings). For each wing, data from four animals are shown in Fig. 7Ai,ii. In eight of the 12 animals, mean burst amplitude was not significantly related to the stroke amplitude of the wing (P>0.05, Fig. 7Bi,ii), while in the remaining four animals, such a correlation was observed (0.45<r<0.56). To examine whether this dependency of tegula burst amplitude on angular velocity was based on a common influence related to the correlation between stroke amplitude and angular velocity reported above, the partial correlation coefficients r* were

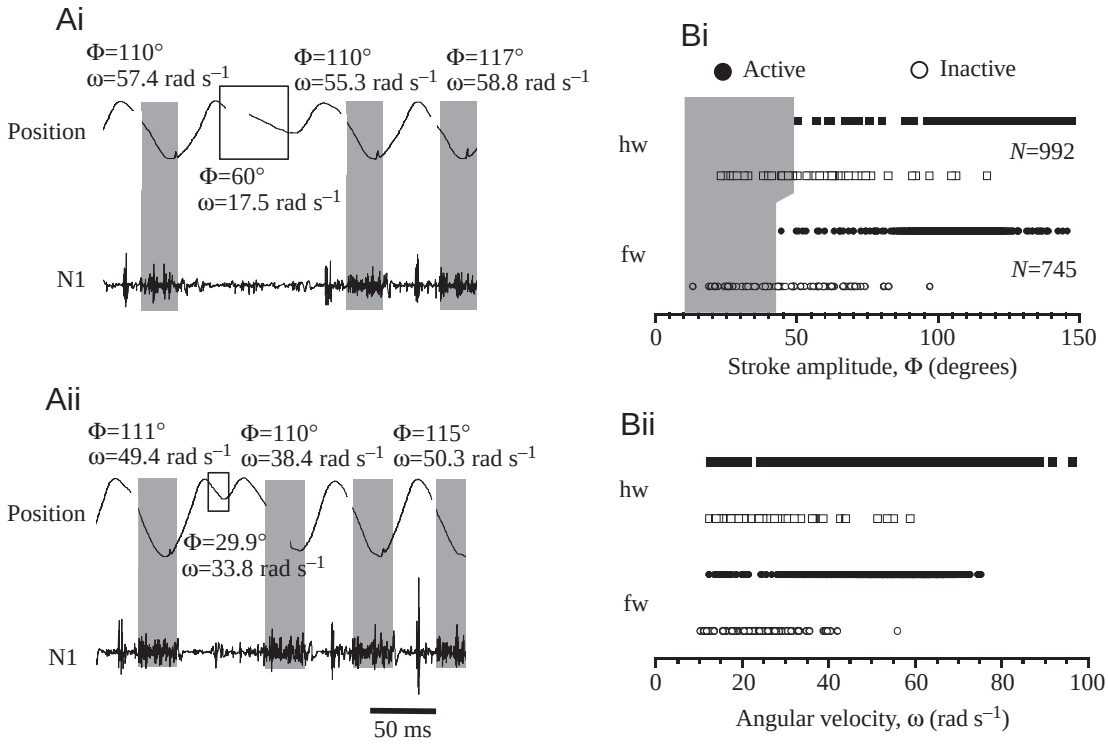

Fig. 8. Downstroke amplitude (Φ) and angular velocity (ω) of the wing as determinants of tegula excitation. (Ai,ii) Two sample recordings from the hindwing organ illustrate failures of the tegula during single wingbeat cycles with incomplete downstroke movements. For each cycle shown, the values of Φ and ω are given. Wing position (top trace) and tegula activity recorded extracellularly from nerve branch N1 (lower trace) are shown. The shaded areas indicate tegula burst duration. (Bi) Excitation of the tegula organs in relation to stroke amplitude. Data for each wing were pooled from eight animals. For the hindwing (hw), no excitation of the tegula was observed during strokes of less than 50 ° in amplitude; in the forewing (fw), the tegula failed at amplitudes of less than 44 ° (illustrated by the shaded area). (Bii) Excitation of the tegula organs in relation to the angular velocity of the downstroke (same data set as above). In both pairs of wings, the tegula organs were active at any given angular velocity within the range of values investigated.

calculated (to remove the interfering variable). In three of the four animals, r^* was significantly different from zero ($P<0.05$, r^* ranging from 0.41 to 0.49), indicating a stronger influence of wing angular velocity on mean burst amplitude than on stroke amplitude.

Effects of tegula ablation on wing stroke amplitude

In five out of nine animals examined, the stroke amplitude (Φ) of the hindwings did not change significantly after removal of the hindwing tegulae (control Φ_c=121.5±21.2 °, deafferented Φ_d=121.6±22.6 °; N=5, $P>0.01$). In these animals, however, tegula removal significantly delayed the start of wing elevation with respect to the preceding downstroke (determined as the phase of elevation onset in the wingbeat cycle defined by the start of the downstroke, ϕ; ϕ_c=0.531±0.033, **r**=0.924; ϕ_d=0.587±0.026, **r**=0.963; $P<0.01$). This indicates that tegula removal in the hindwings prolongs the downstroke interval (cf. Büschges and Pearson, 1991; Wolf, 1993; Fischer and Ebert, 1999). In the remaining animals, the effects of hindwing tegula removal on stroke amplitude were inconsistent: in three of the nine animals, Φ_d decreased (on average by 13 %, $P<0.01$), and Φ_d increased by 9 % in one animal ($P<0.01$). ϕ remained unchanged in three of these animals ($P>0.05$) and decreased in one individual ($P<0.01$). The ablation of the forewing organs had a small and inconsistent effects on forewing stroke amplitude: Φ increased, on average, by 4 % in three out of seven animals (Φ_c=108±9.4 °), remained unchanged in two and decreased in two. In six out of seven animals, ϕ did not change after ablation of the forewing organs (ϕ_c=0.462±0.022, **r**=0.924; ϕ_d=0.464±0.021, **r**=0.963, $P>0.05$; see, for example, Büschges and Pearson, 1991).

Tegula excitation in relation to wing stroke parameters

In both the fore- and hindwings, a failure of tegula discharge was usually observed when the downstroke movement was terminated prematurely (examples are shown for the hindwing in Fig. 8Ai,ii). In both pairs of wings, stroke amplitude (Φ) and angular velocity (ω) were determined for such wingbeat cycles and in a number of cycles where premature termination was suspected. Histograms of these data are given in Fig. 8B. A failure of the hindwing tegula was observed if the amplitude of the wing beat remained within 50 ° of the upper stroke reversal (Fig. 8Bi, indicated by the grey shaded area). This is less than 40 % of the mean wingbeat amplitude (Φ_{hw}=119.9±21.8 °, N=8). Similarly, excitation of the forewing

tegula failed at stroke amplitudes below 44 °, or 40 % of the mean stroke amplitude of the forewing (Φ_{fw}=110.9±18.6 °, *N*=8). Occasional failures were also observed at higher stroke amplitudes for reasons as yet undetermined. In both sets of wings, tegula failure was apparently unrelated to a minimum angular velocity of the downstroke movement (Fig. 8Bii).

Discussion

An understanding of the sensorimotor integration processes that participate in the selection and production of locomotor behaviour requires not only the identification of the response properties of the primary mechanoreceptors (see references in the Introduction), including the complex transduction 'cascade' that underlies the excitation of a particular sensory cell (e.g. Moran et al., 1976), but also a consideration of the possibility that a large population of, possibly different, afferent input fibres might encode particular signals (for an overview, see Sparks et al., 1997).

The present study focuses on an insect mechanosensory organ, the tegula, the knob-shaped cupola of which is integrated into a common ligament attached to the scutum, basalar sclerite, thoracic pleura and leading edge of the wing (Fig. 3). This wing-associated sense organ plays an important role in the generation and modulation of the flight motor pattern. However, in contrast to other wing-related sense organs, which usually consist of one morphological type of mechanoreceptor, the tegula houses two morphologically distinct sensory systems. Each consists of a relatively large number of primary mechanosensory axons, approximately 40 from mechanosensory hairs located on the posterior cupola and approximately 30 scolopidial sensilla from a chordotonal organ attached to the inner surface of the posterior cupola. These sensory cells each project into the central nervous system in a single afferent axon (Kutsch et al., 1980), which makes (excitatory) monosynaptic connections with motoneurons driving the wing elevator muscles (Pearson and Wolf, 1988) and also supplies all known interneurons of the flight oscillator in parallel (see Pearson and Wolf, 1988, 1989).

At present, however, little is known about what wingbeat parameters might be encoded by the tegula organs or how the organ might be activated during flight. To address these questions, the present study employed electrophysiology and high-speed video recordings to monitor the collective activity patterns of tegula afferents, the kinematic movements of the wing and of the tegula organs themselves as well as of the cuticular structures of the wing hinge attached to the tegula organs.

Excitation of the tegula organs during flight

It has been hypothesised that the tegula is excited during flight by the organ touching a membranous fold during the downstroke, probably resulting in the bending of the mechanosensory hairs on the posterior cupola (Kutsch et al., 1980). The high-speed video recordings confirmed that, during the downstroke, the posterior region of the tegula on which the hair plate is located touches a membrane fold located just ventral to the subcosta. This contact is intensified by the anterior deviation of the wing (Fig. 1C) during the downstroke and by the synchronous, posteriorly directed shift of the scutum (Fig. 3). Since the hair plate region was covered partly by the membrane fold itself and partly by the ligament (and, thus, was not visible in the video recordings) when the wing approached its lower reversal position, we were unable to quantify accurately the total time of contact between the hair plate region and the membrane fold from the high-speed recordings. We conclude from our recordings, however, that at least part of the hair plate region touches the membrane fold during approximately half of the cycle period, including one-third of the upstroke interval. The nerve recordings (Figs 2, 6) show that tegula activity starts with a brief delay after the upper stroke reversal, thus roughly matching the time in the cycle when part of the hair plate makes first contact with the membrane fold. Nevertheless, stimulation of the hair plate may not play a key role in tegula excitation because (i) a tegula discharge during the wingbeat cycle cannot be prevented by covering the hair plate with wax (Neumann, 1985) and (ii) tegula bursts reliably terminated at the lower reversal point of the wing (Fig. 2), i.e. at a time when the hair plate was still in contact with the membrane fold.

The mechanisms that, apparently, limit the tegula discharge to the downstroke interval are not clear at present. The obvious coincidence between the posterior stroke deviation, which starts when the wing passes its lower stroke reversal (Fig. 4B), and tegula burst termination might indicate that the tegula is also sensitive to wing motion in a plane perpendicular to the stroke plane and, thus, that the anterior stroke deviation during the downstroke (see Fig. 4B) might limit tegula activity to the downstroke interval. However, this hypothesis now needs to be addressed by further experimentation.

For both wings, a failure in tegula excitation was almost exclusively observed during stroke cycles in which the wing did not reach its normal lower reversal point (Fig. 8B). However, tegula failure was not restricted to cycles in which the angular velocity was particularly low (Fig. 8B). In addition, moving the wing passively at angular velocities far below those observed during active flight, but at comparable amplitudes, activated the tegula organs (see Fig. 2 in Fischer and Ebert, 1999). This indicates that excitation of the tegula relies on the wing passing a 'critical' position during the downstroke rather than the wing reaching a certain angular velocity (Fig. 8Bii). Together with the observations of Neumann (1985), this suggests that the response of position-sensitive afferents in the chordotonal organ of the tegula might play a role in the activation of the organ during the wing stroke.

The pterothoracic scuta are attached to each other by a flexible ligament. The two scuta move posteriorly at different phases during the downstroke, but they shift anteriorly almost in synchrony during the upstroke (Fig. 3). The hindwing tegula is integrated into this ligament, which inserts in a mesothoracic fold located posteriorly between the scutum and the dorsal border of the epimeron. One might expect, therefore, that

hindwing tegula activity would be affected by the kinematics of the forewing. However, we found no indication of a mechanical influence of the mesothoracic scutum on hindwing tegula activity and *vice versa*. Apparently, the two tegula organs are functionally quite separate.

Relationship between wing stroke parameters and tegula activity

The mechanical elements of the locust thorax and wing hinge are tightly coupled and move in strict phase relationships during flight (e.g. Fig. 3). The movement of these elements, to which the tegula organ is attached by a common ligament, results in the rotational and tilting movements of this organ, which occur at stable phase values with respect to wing movement (Fig. 4). Both the latency of tegula activity with respect to the onset of the wing downstroke and the burst duration decrease when the downstroke interval is reduced with increasing wingbeat frequency (Figs 5, 6). This implies that the tegula organs are activated at an almost constant phase during the wingbeat cycle (Fig. 6; Table 1). These observations are in accord with the phase-locked kinematics of the organ's movements.

The present results thus seemingly disagree with previous findings suggesting a relatively constant latency of tegula discharge, at least at lower wingbeat frequencies (Wolf and Pearson, 1988). However, latency was determined with respect to the activity of single wing depressor muscles (first basalar or subalar) in previous studies, and the relationship between the activity of a particular muscle and wing movement can be variable (Wilson and Weis-Fogh, 1962; Pfau, 1978, 1982; Möhl, 1985, 1988). Evaluation of the present data set with regard to first basalar muscle activity indeed demonstrated considerable variability between the individuals tested, including, almost equally, no, positive or negative relationships between latency and cycle period (data not shown). A variable discharge pattern was observed in particular in the first basalar muscle, which is involved in a number of tasks (e.g. flight steering, Zarnack and Möhl, 1977; Baker, 1979; climbing flight, Fischer, 1998; Fischer and Kutsch, 1999; adjustment of the angular setting of the wing, Pfau, 1978, 1982). The quantitative data presented by Wolf and Pearson (1988) were from just one animal, and the slope of the relationship between latency and cycle period, although small (approximately 0.1; H. Wolf and K. G. Pearson, unpublished data), is well within the range of slopes observed in the present study (data not shown, Table 1). The effects of the tegula on the flight motor pattern reported previously (Wolf and Pearson, 1988; Fischer and Ebert, 1999) thus appear to result to a large extent from the constant delay required to elicit elevator activity in response to a tegula discharge, particularly at lower wingbeat frequencies (Wolf, 1993), rather than from a constant latency of tegula activation (see also the effects of tegula ablation reported above).

Key parameters of tegula discharge, such as latency and phase (Fig. 6), duration (Fig. 5) and the mean amplitude of the tegula burst (Fig. 7), were related to the stroke amplitude, downstroke interval and angular velocity of the wing, which are important for aerodynamic force production during flight (e.g. Ellington, 1984; Lehmann and Dickinson, 1997, 1998; Thüring, 1986).

Apart from the fact that a minimum amplitude seems to be required for tegula activation (Fig. 8), stroke amplitude does not appear to play an important role in determining the pattern of tegula discharge during flight since the duration, the latency and the amplitude of the tegula bursts were not significantly related to the amplitude of the wing stroke (Figs 5B, 6B, 7B). Furthermore, removal of the tegula organs had no consistent, if any, effect on stroke amplitude in either pair of wings.

In contrast, the latency and duration of the tegula discharge were significantly related to the downstroke interval and, thus, to the cycle period, since these two parameters are correlated during flight (Table 1; see also Wolf, 1993). The dependency of the duration and latency of tegula discharge on the downstroke interval is evident when considering the fact that the tegula is excited by (e.g. Wolf and Pearson, 1988) (Fig. 8Ai) and is active during the downstroke, and it suggests that the tegula encodes parameters of the downstroke such as timing (Wolf, 1993) and velocity (see also Figs 5C, 6C).

In both sets of wings, latency (Fig. 6C), burst duration (Fig. 5C) and burst amplitude (Fig. 7A) depend on the angular velocity of the wing. The relationship between latency and angular velocity is non-linear. Towards higher angular velocities, latency approaches or reaches a minimum value and often stays near this minimum if angular velocity increases further. The minimum is reached between approximately 45 and 75 $rad\,s^{-1}$. The corresponding wingbeat frequencies are between approximately 15 and 19 Hz, i.e. they mark the lower limit of frequencies observed during free flight. The latency of the tegula discharge thus appears to be kept within a narrow range during normal flight, indicating that a feedback loop is functioning. Furthermore, the tegula organs are sensitive to a very wide range of angular velocities (Fig. 8), including very low values (e.g. 2–5 $rad\,s^{-1}$) that are not observed during flight (data shown in and extracted from Fig. 2 in Fischer and Ebert, 1999). In principle, angular velocity could be adjusted by controlling stroke amplitude or cycle period or both. However, in 85 % of the animals examined, angular velocity was (negatively) related to the cycle period (Table 1), while in only 60 % of the locusts was it (positively) related to stroke amplitude (data not shown). It appears, therefore, that angular velocity is primarily related to wingbeat frequency.

The above conclusions are based on the changes in the collective activity of the tegula afferents with respect to variation in particular wingbeat parameters. It has previously been suggested that the tegula might work as a functional unit since the two sensory systems in the tegula are in close vicinity to each other (Kutsch et al., 1980). However, since the tegula consists of a large number of afferents (in contrast to other wing-associated sensory organs, e.g. the single-cell stretch receptor), there is the distinct possibility of different response properties and range fractionation (for reviews, see Field and Matheson, 1998; Newland et al., 1995; Neumann, 1985)

among the 70–80 sensory cells of the tegula. This might allow population-coding of wingbeat parameters, although at present this possibility must remain speculative because of the absence of data concerning tegula receptor physiology or the the specificity of the central connections of different receptor cell types.

In the present study, a meaningful distinction of different spike amplitudes, or discharge properties of different axon populations, was not possible because of the rather homogeneous distribution of both spike amplitudes and discharge characteristics in the compact tegula bursts (data not shown, but see Fig. 2). Even in the few cases where large, small and sometimes intermediate spike amplitudes could be differentiated in the tegula discharge, these groups of sensory axons had very similar discharge patterns (data not shown).

The locust pterothorax is a compact mechanical structure composed of a large number of coupled cuticular elements that move in strict phase relationships during flight (e.g. Fig. 3). The mechanical composition and properties of the pterothorax (including flight musculature) both determine, to a major extent, the complex three-dimensional wing movements (Pfau, 1978, 1982) and limit the power output of the flight oscillator through their mechanical damping properties (Roeder, 1951; Soltavalta, 1952). A more global assessment of flight performance should consider at least two points. First, the activation phase of the flight muscles, which controls their mechanical power output (e.g. Stevenson and Josephson, 1990), and in turn is translated into basic flight parameters, such as wingbeat frequency, stroke amplitude, the angular velocity of the wing and finally into aerodynamic force production, should be examined. Second, an appropriate tuning of these flight parameters may be important not only for flight performance *per se* but also in the context of a possible resonance stabilisation of the flight oscillator (Greenwald, 1960; Scharstein, 1998a,b).

Insects need to activate their flight muscles at appropriate times and phases to generate a functional flight pattern under a variety of conditions, e.g. during changes in stroke frequency. This provides a direct functional context for wingbeat-synchronous (i.e. phase-locked, Fig. 6) sensorimotor pathways, such as that involving the tegula, which are important in flight motor control (e.g. Wendler, 1974; Möhl, 1985; Wolf and Pearson, 1988; Wolf, 1993; Fischer and Ebert, 1999). Thus, the respective sense organs may serve to monitor, and control, the appropriate tuning of critical flight variables, e.g. the angular velocity of the wing, which plays an important role in aerodynamic performance (e.g. Ellington et al., 1996; Lehmann and Dickinson, 1998; Dickinson et al., 1999). If there is not just a correlation between particular parameters of wing movement and tegula discharge, but if this correlation is non-linear and a preferred parameter combination is maintained during normal flight (e.g. the phase of tegula activation during the cycle or the relationship between latency and angular velocity, Fig. 6), this may indicate that a feedback loop is involved. Tegula afferent pathways might thus be part of a feedback loop controlling not only the basic flight motor pattern (Wolf and Pearson, 1988) but also the angular velocity of the downstroke, with the variations in tegula activity serving as error signals for these control loops. However, experiments demonstrating conclusively such feedback loops can be obtained only by examining the control circuit in cybernetic experiments (e.g. Wendler, 1974).

We gratefully acknowledge the Fachbereich Biologie, Universität Konstanz (Germany), for providing the digital high-speed video system (funded by an HBFG grant to the University). We thank W. Kutsch (Universität Konstanz) for providing laboratory space and basic equipment during the initial parts of the study. T. Breithaupt (Universität Konstanz) generously provided a variety of special equipment. We are grateful to C. Graef (Universität Köln, Germany) for technical assistance and to H. Scharstein and G. Wendler (Universität Köln) for valuable discussions. Special thanks are due to W. J. Heitler (University of St Andrews, Scotland) for a custom-made upgrade of DataView. We thank three anonymous referees for valuable comments and suggestions regarding the analysis and interpretation of our data, and S. D. Merrywest, D. L. McLean and R. J. Chapman (University of St Andrews) for critically reading the manuscript.

References

Albrecht, F. O. (1953). *The Anatomy of the Migratory Locust.* London: The Athalone Press.

Baker, P. S. (1979). The role of forewing muscles in the control of direction in flying locusts. *J. Comp. Physiol. A* **131**, 59–66.

Baker, P. S. and Cooter, R. J. (1979). The natural flight of the migratory locust, *Locusta migratoria*. I. Wing movements. *J. Comp. Physiol. A* **131**, 79–87.

Bässler, U. (1983). *Neural Basis of Elementary Behaviour in Stick Insects* (ed. V. Braitenberg), pp. 1–69. Berlin: Springer-Verlag.

Batschelet, E. (1981). *Circular Statistics in Biology*. London, New York: Academic Press.

Burns, M. D. (1974). Structure and physiology of the locust femoral chordotonal organ. *J. Insect Physiol.* **29**, 1319–1339.

Büschges, A. (1994). The physiology of sensory cells in the ventral scoloparium of the stick insect femoral chordotonal organ. *J. Exp. Biol.* **189**, 285–292.

Büschges, A. and El Manira, A. (1998). Sensory pathways and their modulation in the control of locomotion. *Curr. Opin. Neurobiol.* **8**, 733–739.

Büschges, A. and Pearson, K. G. (1991). Adaptive modifications in the flight system of the locust after the removal of wing proprioceptors. *J. Exp. Biol.* **157**, 313–333.

Campbell, J. (1961). The anatomy of the nervous system of the mesothorax of *Locusta migratoria*. *Proc. Zool. Soc. Lond.* **137**, 403–432.

Chau, C., Barbeau, H. and Rossignol, S. (1998). Effects of intrathecal alpha1- and alpha2-noradrenergic agonists and norepinephrine on locomotion in chronic spinal cats. *J. Neurophysiol.* **79**, 2941–2963.

Dean, J. and Wendler, G. (1983). Stick insect locomotion on a walking wheel: interleg coordination of leg position. *J. Exp. Biol.* **110**, 75–94.

Dickinson, M., Lehmann, F.-O. and Sane, S. (1999). Wing rotation and the aerodynamic basis of insect flight. *Science* **284**, 1954–1960.

Dugard, J. J. (1967). Directional change in flying locusts. *J. Insect Physiol.* **13**, 1055–1063.

Ellington, C. P. (1984). The aerodynamics of insect flight. III. Kinematics. *Phil. Trans. R. Soc. Lond. B* **305**, 41–78.

Ellington, C. P., van den Berg, C., Willmott, A. P. and Thomas, A. L. R. (1996). Leading-edge vortices in insect flight. *Nature* **384**, 626–630.

Field, L. H. and Matheson, T. (1998). Chordotonal organs of insects. *Adv. Insect Physiol.* **27**, 1–228.

Field, L. H. and Pflüger, H.-J. (1989). The femoral chordotonal organ: a

bifunctional orthopteran (*Locusta migratoria*) sense organ? *Comp. Biochem. Physiol.* **93**, 729–743.
Fischer, H. (1998). *Untersuchungen zur Verhaltensphysiologie frei fliegender Heuschrecken unter Einsatz von Telemetrie*, vol. 347. Allensbach: UFO Atelier & Verlag GmbH.
Fischer, H. and Ebert, E. (1999). Tegula function during free locust flight in relation to motor pattern, flight speed and aerodynamic output. *J. Exp. Biol.* **202**, 711–721.
Fischer, H. and Kutsch, W. (1999). Timing of elevator activity during climbing in free locust flight. *J. Exp. Biol.* **202**, 3575–3586.
Gettrup, E. (1966). Sensory regulation of wing twisting in locusts. *J. Exp. Biol*. **44**, 1–16.
Greenwald, C. H. (1960). The wings of insects and birds as mechanical oscillators. *Proc. Am. Phil. Soc*. **104**, 605–611.
Hofmann, T. and Koch, T. U. (1985). Acceleration receptors in the femoral chordotonal organ of the stick insect, *Cuniculina impigra*. *J. Exp. Biol*. **114**, 225–237.
Josephson, R. K. (1985). Mechanical power output from striated muscle during cyclic contraction. *J. Exp. Biol.* **114**, 493–512.
Kent, K. S. and Griffin, L. M. (1990). Sensory organs of the thoracic legs of the moth *Manduca sexta*. *Cell Tissue Res*. **259**, 209–223.
Kittmann, R. and Schmitz, J. (1992). Functional specialisation of the scoloparia of the femoral chordotonal organ in stick insect. *J. Exp. Biol*. **173**, 91–108.
Kniazeva, N. I. (1970). Receptors of the wing apparatus regulating the flight of the migratory locust, *Locusta migratoria* L. (Orthoptera, Acrididae). *Entomol. Rev*. **49**, 311–317.
Kutsch, W., Hanloser, H. and Reinecke, M. (1980). Light- and electron-microscopic analysis of a complex sense organ: the tegula of *Locusta migratoria*. *Cell Tissue Res.* **210**, 461–478.
Lehman, F.-O. and Dickinson, M. (1997). The changes in power requirements and muscle efficiency during elevated force production in the fruit fly *Drosophila melanogaster*. *J. Exp. Biol.* **200**, 1133–1143.
Lehman, F.-O. and Dickinson, M. (1998). The control of wing kinematics and flight forces in fruit flies (*Drosophila* spp.). *J. Exp. Biol.* **201**, 385–401.
Matheson, T. (1990). Responses and location of neurones in the locust metathoracic femoral chordotonal organ. *J. Comp. Physiol. A* **166**, 915–927.
Matheson, T. and Field, L. (1995). An elaborate tension receptor system highlights sensory complexity in the hind leg of the locust. *J. Exp. Biol.* **198**, 1673–1689.
Möhl, B. (1985). The role of proprioception in locust flight. I. Asymmetry and coupling within the time pattern of motor units. *J. Comp. Physiol. A* **156**, 93–101.
Möhl, B. (1988). Short-term learning during flight control in *Locusta migratoria*. *J. Comp. Physiol. A* **163**, 803–812.
Moran, D. T., Rowley, J. C., Zill, S. N. and Valera, F. G. (1976). The mechanism of sensory transduction in a mechanoreceptor. *J. Cell Biol*. **71**, 832–847.
Mücke, A. (1991). Innervation pattern and sensory supply of the midleg of the locust *Schistocerca gregaria* (Insecta, Orthoptera). *Zoomorphologie* **100**, 175–187.
Neumann, L. (1985). Experiments on tegula function for flight coordination in the locust. In *Insect Locomotion* (ed. M. Gewecke and G. Wendler), pp. 149–156. Berlin, Hamburg: Paul Parey.
Newland, P. L., Watkins, B., Emptage, N. J. and Nagayama, T. (1995). The structure, response properties and development of a hair plate on the mesothoracic leg of the locust. *J. Exp. Biol.* **198**, 2397–2404.
Pearson, K. G. and Wolf, H. (1988). Connections of hindwing tegulae with flight neurones in the locust, *Locusta migratoria*. *J. Exp. Biol*. **135**, 381–409.
Pearson, K. G. and Wolf, H. (1989). Timing of forewing elevator activity during flight in the locust. *J. Comp. Physiol. A* **165**, 217–227.
Pfau, H. K. (1978). Funktionsanatomische Aspekte des Insektenfluges. *Zool. Jb. Anat.* **99**, 99–108.
Pfau, H. K. (1982). Mechanik und sensorische Kontrolle der Flügel-Pronation und -Supination. In *Biona Report* 1 (ed. W. Nachtigall), pp. 61–77. Stuttgart, New York: Gustav Fischer.
Pfau, H. K. and Koch, T. U. (1994). Functional morphology of singing in the cricket. *J. Exp. Biol*. **195**, 147–167.
Pflüger, H.-J., Bräunig P. and Hustert, R. (1981). Distribution and specific central projections of mechanoreceptors in the thorax and proximal leg joints of locusts. II. The external mechanoreceptors: Hair plates and tactile hairs. *Cell Tissue Res*. **216**, 79–96.
Reye, D. N. and Pearson, K. G. (1988). Entrainment of the locust central flight oscillator by wing stretch receptor stimulation. *J. Comp. Physiol. A* **164**, 15–24.
Roeder, K. D. (1951). Movements of the thorax and potential changes in the thoracic muscles during flight. *Biol. Bull*. **100**, 95–113.
Sachs, L. (1978). *Angewandte Statistik*. Fifth edition. Berlin: Axel Springer.
Sane, S. P. and Dickinson, M. H. (2001). The control of flight force by a flapping wing: lift and drag production. *J. Exp. Biol.* **204**, 2607–2626.
Scharstein, H. (1998a). Ein Piezo-Flugelantrieb zur Untersuchung der Biophysik und Aerodynamik des Insektenfluges. In *Biona Report* 13 (ed. W. Nachtigall and A. Wisser), pp. 189–191. Stuttgart, Jena, Lübeck, Ulm: Gustav Fischer.
Scharstein, H. (1998b). Kräfte- und Leistungsbilanz bei der künstlichen Schlagbewegung einzelner Insektenflügel. In *Biona Report* 13 (ed. W. Nachtigall and A. Wisser), pp. 257–270. Stuttgart, Jena, Lübeck, Ulm: Gustav Fischer.
Snodgrass, R. E. (1929). The thoracic mechanism of a grasshopper and its antecedents. *Smithson. Misc. Collns*. **82**, 1–111.
Soltavalta, O. (1952). The essential factor regulating the wing stroke frequency of insects in wing mutilation and loading experiments and in experiments at subatmospheric pressure. *Ann. Zool. Vanamo* **15**, 1–68.
Sparks, D. L., Kristan, W. B. and Shaw, B. K. (1997). The role of population coding in the control of movement. In *Neurons, Networks and Motor Behaviour* (ed. P. S. G. Stein, S. Grillner, A. I. Selverston and D. G. Stuart), pp. 21–32. Cambridge, MA: The MIT Press.
Stevenson, R. D. and Josephson, R. K. (1990). Effects of operating frequency and temperature on mechanical power output from moth flight muscle. *J. Exp. Biol*. **149**, 61–78.
Thüring, D. A. (1986). Variability of motor output during flight steering in locusts. *J. Comp. Physiol. A* **158**, 653–664.
Thurm, U. (1982). Biophysik sensorischer Mechanismen. In *Biophysik* (ed. W. Hoppe, W. Lohmann, H. Markl and H. Ziegler), pp. 681–696. Berlin, Heidelberg: Springer.
Thurm, U. (1984). Beiträge der Ultrastrukturforschung zur Aufklärung sensorischer Mechanismen. *Verh. Dt. Zool. Ges.* **77**, 89–103.
von Helversen, O. and Elsner, N. (1977). The stridulatory movements of acridid grasshoppers recorded with an opto-electronic device. *J. Comp. Physiol. A* **122**, 53–64.
Wendler, G. (1974). The influence of proprioceptive feedback on locust flight coordination. *J. Comp. Physiol. A* **88**, 173–200.
Wilson, D. M. and Weis-Fogh, T. (1962). Patterned activity of co-ordinated motor units, studied in flying locusts. *J. Exp. Biol*. **39**, 643–667.
Wolf, H. (1993). The locust tegula: significance for flight rhythm generation, wing movement control and aerodynamic force production. *J. Exp. Biol.* **182**, 229–253.
Wolf, H. and Pearson, K. G. (1987a). Intracellular recordings from interneurons and motoneurons in intact flying locusts. *J. Neurosci. Meth.* **21**, 345–354.
Wolf, H. and Pearson, K. G. (1987b). Comparison of motor patterns in the intact and deafferented flight system of the locust. I. Electromygraphic analysis. *J. Comp. Physiol. A* **160**, 259–268.
Wolf, H. and Pearson, K. G. (1988). Proprioceptive input patterns elevator activity in the locust flight system. *J. Neurophysiol*. **59**, 1831–1853.
Wong, R. K. S. and Pearson, K. G. (1976). Properties of the trochanteral hair plate and its function in the control of walking in the cockroach. *J. Exp. Biol*. **64**, 233–249.
Yack, J. E. and Fullard, J. H. (1993). What is an insect ear? *Ann. Ent. Soc. Am.* **86**, 677–682.
Zarnack, W. and Möhl, B. (1977). The activity of the direct downstroke muscles of *L. migratoria* during steering behaviour in flight. I. Patterns of time shift. *J. Comp. Physiol. A* **118**, 235–247.
Zarnack, W. and Wortmann, W. (1989). On the so-called constant-lift reaction of migratory locusts. *J. Exp. Biol.* **147**, 111–124.
Zill, S. N. (1985). Plasticity and proprioception in insects. I. Reponses and cellular properties of individual receptors of the locust metathoracic femoral chordotonal organ. *J. Exp. Biol*. **116**, 435–461.